Sensors and Materials, Vol. 28, No. 11 (2016) 1219–1228
MYU Tokyo

S & M 1283

Sensing of Soot Oxidation by Using Combustion-Type Sensor with Ag-Supported Catalyst

Hongcheng Ruan, Maiko Nishibori,* Tsutomu Itou,
Yoshihiko Sadaoka,[1] and Yasutake Teraoka

Department of Molecular and Material Sciences, Interdisciplinary Graduate School of Engineering Sciences,
Kyushu University, Kasuga, Fukuoka 816-8580, Japan
[1]Department of Materials Science and Biotechnology, Graduate School of Science and Engineering,
Ehime University, 3 Bunkyo-cho, Matsuyama, Ehime 790-8577, Japan

(Received June 10, 2016; accepted August 3, 2016)

Keywords: particulate matter, oxidation, catalyst, combustion-type sensor

Soot-sensing properties of the combustion-type sensor coated with Ag-supported catalysts (Ag/TiO_2, $Ag/\alpha\text{-}Al_2O_3$, and Ag/CeO_2) were investigated. The catalyst with a high carbon black (CB) oxidation activity in the tight contact (TC) mode had a high response speed, although the response speed had no relationship with the CB oxidation activity in the loose contact (LC) mode. Moreover, the difference in CB oxidation activities between TC and LC modes was consistent with the difference in response speed between V_{10} and V_{50}, where V_{10} and V_{50} indicate the response speed of the CB oxidation at 10 and 50% of total output voltage. The catalyst with high intrinsic CB combustion activity improves the response property at initial combustion. On the other hand, the catalyst with the CB combustion activity, which does not depend on the contact state between the CB and the catalyst, improves the response property at later combustion.

1. Introduction

Particulate matter (PM), which mainly consists of soot and soluble organic fraction (SOF) from diesel engines, is one of the main pollutants causing the PM2.5 problem, along with other serious environmental and health problems.[1–3] Generally, improving fuel quality, boosting engine performance, and developing diesel exhaust after-treatment systems are the main ways of reducing PM emissions from diesel vehicles. Research on diesel exhaust after-treatment is a promising solution. The catalysed diesel particulate filter (C-DPF) is commonly regarded as the most effective technology for reducing PM emissions from diesel engines, where the PM is trapped and oxidized using a catalyst at low temperatures.[4–6] Therefore, to guarantee the efficient and stable operation of a diesel engine system with C-DPF after-treatment, on-board PM monitoring technology is required.[3,7,8]

For this reason, several soot detection technologies have been proposed by researchers in the last few decades. Potentiometric and amperometric soot sensors based on an oxide ion conductor (zirconia) and electrical insulator were proposed by Vogel and colleagues[8,9] and Moss and colleagues,[10–12] and these can be used for *in situ* measurements of soot concentration. Sensors based on the

*Corresponding author: e-mail: nishibori.maiko.511@m.kyushu-u.ac.jp

ISSN 0914-4935

electromagnetic wave method, which includes radio-frequency (RF)[13,14] and optical waves in terms of changing the light transmission, scattering or extinction, have also been used to monitor PM concentration.[15–18] In addition, a series of PM sensors dependent on polarization resistance resulting from a four-electron electrochemical reaction ($C + H_2O \rightarrow CO_2 + 4H^+ + 4e^-$) by utilizing a solid electrolyte as well as an electrocatalyst were proposed by Hibino and colleagues.[7,19–21]

Ag is well known as an efficient partial oxidation catalyst. For instance, Ag has been used industrially for the epoxidation of ethylene[22,23] and the oxdehydrogenation of methanol to formaldehyde.[24–26] In addition, Ag is well-used for NO_x abatement,[27,28] and the oxidation of ammonia,[29] methane,[30] carbon monoxide,[31] organic volatile compounds.[32] Ag with support materials such as ZrO_2, TiO_2, Al_2O_3 and CeO_2 also showed remarkable performance for diesel soot oxidation.[33–36]

In this study, we evaluate the soot oxidation activities of Ag-supported catalysts (Ag/TiO_2, Ag/α-Al_2O_3, and Ag/CeO_2) and discuss the soot sensing properties of the catalytic combustion-type sensor, which converts oxidation heat into an electric signal, with these catalysts. Additionally, we evaluate the relationship between the sensing properties and the soot oxidation activities of the catalysts.

2. Experimental Procedure

2.1 Catalysts for soot oxidation

TiO_2 [JRC-TiO-4(2), Catalysis Society of Japan], α-Al_2O_3 (Taimei Chemicals), and CeO_2 (JRC-CEO-2, Catalysis Society of Japan) were used as the catalyst supports. To change the particle size, CeO_2 was calcined at 500 and 1300 °C. Ag-loaded catalysts were prepared by ordinary impregnation of the catalyst support material with an aqueous solution of silver nitrate [$AgNO_3$ (Kishida Chemical)]. The Ag content in the catalyst was fixed at 4.5 wt% on the basis of our previous research.[36] The suspended solutions were evaporated to dryness under stirring at 350 °C and then baked at 350 °C for 2 h, followed by calcination at 500 °C for 5 h in air.

The Brunauer, Emmett, and Teller (BET) specific surface areas of the catalysts were measured by nitrogen adsorption at 77 K (BELSORP-mini gas adsorption analyzer, BEL Japan, Inc.). Thermogravimetry (TG) and differential thermal analysis (DTA) measurements (TG/DTA 7300, HITACHI) were carried out to evaluate the soot oxidation activity of the catalysts at a heating rate of 10 °C min^{-1} from 30 to 800 °C in synthetic air (21 vol.% O_2 and 79 vol.% N_2, 100 ml min^{-1}) after the pre-heat treatment at 120 °C for 2 h. In this study, commercially available carbon black (CB, Sigma-Aldrich), which has a particle size of 5 μm, was used as a substitute for soot. All the catalysts and CB were mixed by grinding together in a mortar with pestle and spatula for 10 min, denoted as tight contact (TC) mode and loose contact (LC) mode, respectively.

2.2 Fabrication and evaluation of sensor

The sensor element and fabrication of the sensing device are shown in Fig. 1. Sensor elements, a combination of a Pt coil and γ-Al_2O_3 bead, were coated with a slurry of Ag/TiO_2, Ag/α-Al_2O_3, and Ag/CeO_2 catalysts, respectively. They were then heated at 600 °C for 2 h in air by using an internal Pt heater of the sensor element to remove the binder resin. After that, the CB slurry was coated on the catalyst-coated sensor element, followed by heating at 200 °C for 2 h in air. The catalyst

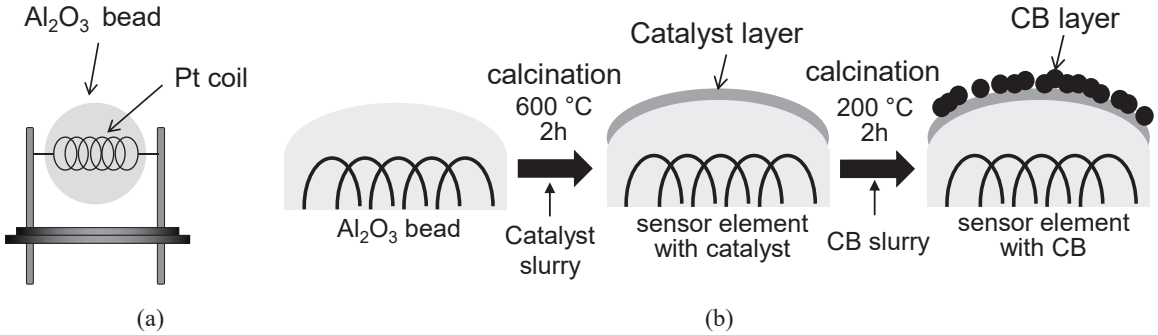

Fig. 1. Schematic of (a) sensor element and (b) fabrication of sensing device.

slurry was prepared by mixing catalysts and terpineol ($C_{10}H_{18}O$, Wako) at a weight ratio of 9:1 for 3 min using a mixer (AR-100, Thinky) for 3 min. On the other hand, the CB slurry was prepared by mixing CB and terpineol at a weight ratio of 12:1.

The sensing principle and measurement system used in this study were the same as those described in previous research.[3] A Wheatstone bridge circuit, which includes a sensor element coated with the catalyst and a reference element without the catalyst, was employed. The temperature dependence of output voltage for CB oxidation was measured from 50 to 600 °C at intervals of 50 °C in synthetic air at a gas flow rate of 50 ml min^{-1}. The temperature of the sensor element was controlled and kept constant for 3 min at each measurement temperature by the Pt heater. On the other hand, the response property was investigated at a constant temperature of 600 °C by changing the gas from N_2 to air.

3. Results and Discussion

3.1 CB oxidation activity of Ag/TiO_2, $Ag/\alpha\text{-}Al_2O_3$, and Ag/CeO_2 catalysts

The TG-DTA curves for CB oxidation of Ag/TiO_2, $Ag/\alpha\text{-}Al_2O_3$, and Ag/CeO_2 catalysts in TC and LC modes are shown in Fig. 2. Table 1 shows the specific surface area and CB oxidation activities in TC and LC modes. T_{ig} and T_{max} indicate the starting temperature of weight loss in the TG curve and the peak temperature of the DTA curve, respectively.

In the TC mode, the Ag/TiO_2 catalyst showed higher CB oxidation activity, which means lower oxidation temperatures of T_{ig} and T_{max}, than the $Ag/\alpha\text{-}Al_2O_3$ and Ag/CeO_2 catalysts. Although both $Ag/\alpha\text{-}Al_2O_3$ and Ag/CeO_2 catalysts showed the same T_{ig}, T_{max} with the $Ag/\alpha\text{-}Al_2O_3$ catalyst was lower than that with the Ag/CeO_2 catalyst and had a sharp DTA peak, which means quick combustion of CB. In the LC mode, both $Ag/\alpha\text{-}Al_2O_3$ and Ag/CeO_2 catalysts showed the same T_{ig} and T_{max}, and this suggests that the CB oxidation activities of these catalysts are not different in the state in which CB and the catalysts contacted weakly. Furthermore, the CB oxidation activity of the Ag/TiO_2 catalyst was low and T_{max} was higher than those of the $Ag/\alpha\text{-}Al_2O_3$ and Ag/CeO_2 catalysts.

The Ag/TiO_2 catalyst has an intrinsically high activity for CB oxidation and showed a large difference in catalytic activity between the TC and LC modes. On the other hand, the Ag/CeO_2 catalyst is different from the other two catalysts and showed similar CB oxidation activity between the TC and LC modes.

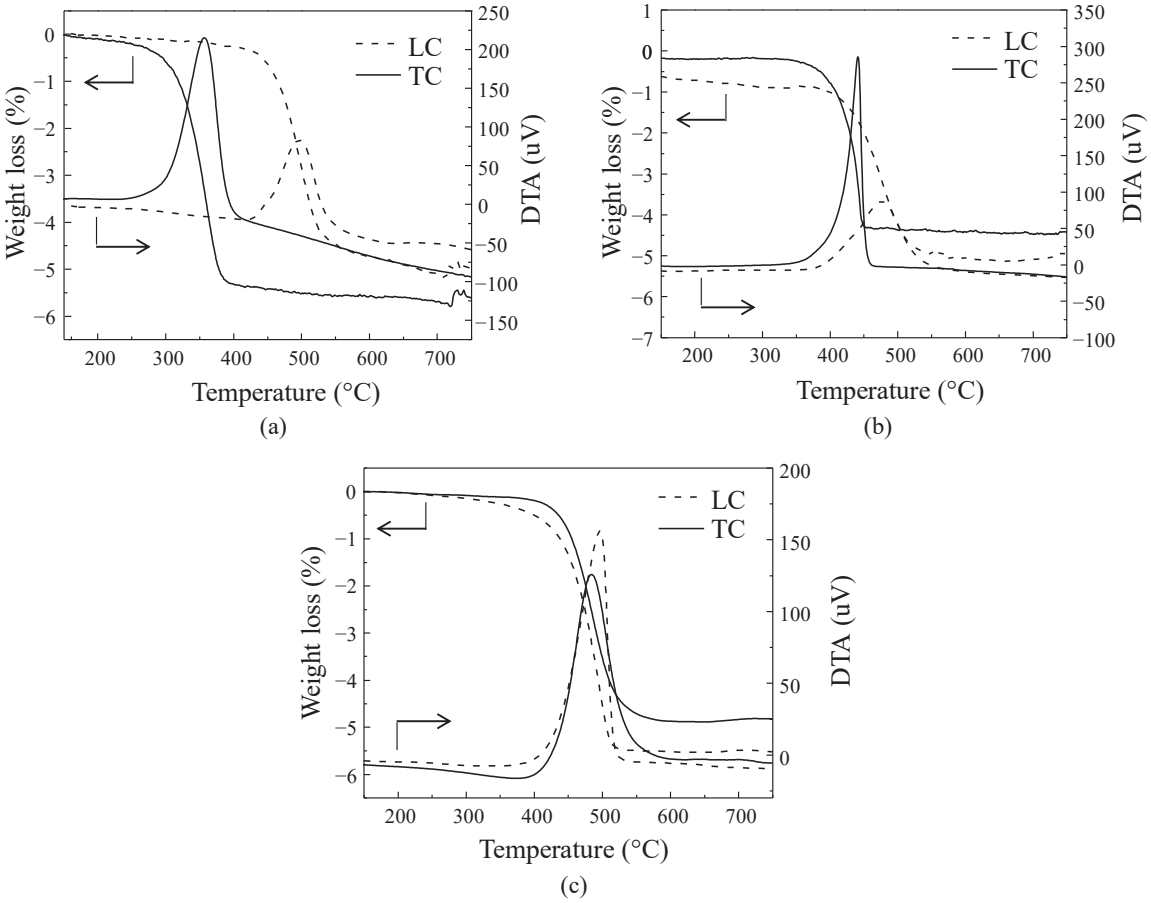

Fig. 2. TG-DTA curves for CB oxidation with (a) Ag/TiO_2, (b) $Ag/\alpha\text{-}Al_2O_3$, and (c) Ag/CeO_2 catalysts in TC and LC modes.

Table 1
Specific surface area and catalytic performances for CB combustion in both TC and LC modes.

Catalyst	S_{BET} (m^2g^{-1})[a]	CB oxidation performance (°C)[b]				
		TC mode		LC mode		ΔT_{max}
		T_{ig}	T_{max}	T_{ig}	T_{max}	
Ag/TiO_2	11.2	268	357	376	497	140
$Ag/\alpha\text{-}Al_2O_3$	5.6	340	442	404	480	38
Ag/CeO_2	0.5	346	492	405	484	8

[a]Specific surface area.

[b]T_{ig} starting temperature of weight loss in TG curve; T_{max} peak temperature of DTA curves; ΔT_{max} difference of ΔT_{max} between TC and LC modes.

3.2 Temperature dependence of output voltage for CB oxidation using sensor elements

Figure 3 shows the temperature dependence of output voltage for CB oxidation using the sensor elements coated with Ag/TiO_2, $Ag/\alpha\text{-}Al_2O_3$, and Ag/CeO_2 catalysts. Here, the increase in output voltage corresponds to CB combustion with different catalysts. For the sensor element with the Ag/TiO_2 catalyst [Fig. 3(a)], the output voltage began to increase from 300 °C and then increased

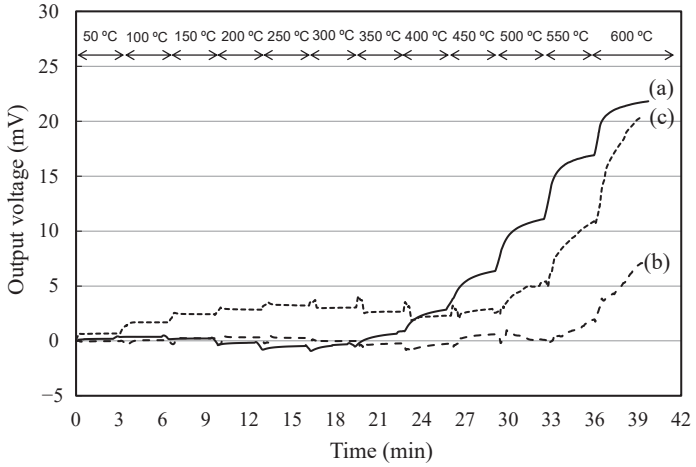

Fig. 3. Temperature dependence of output voltage for CB oxidation using sensor elements with (a) Ag/TiO_2, (b) $Ag/\alpha\text{-}Al_2O_3$, and (c) Ag/CeO_2 catalysts.

rapidly with increasing temperature owing to the CB oxidation reaction with the increase in CB combustion heat. Moreover, for the sensor elements with $Ag/\alpha\text{-}Al_2O_3$ [Fig. 3(b)] and Ag/CeO_2 [Fig. 3(c)], the output voltage began to increase from about 450 and 400 °C, respectively.

The increase in the output voltage of the sensor elements with Ag/TiO_2, Ag/CeO_2, and $Ag/\alpha\text{-}Al_2O_3$ catalysts under constant temperature, ΔV, which was estimated from Fig. 3, is shown in Fig. 4(a) as a function of temperature. The ΔV corresponds to the combustion heat of CB, which indicates the amount of combusted CB on the element. The ΔV of the sensor element with the Ag/TiO_2 catalyst began to increase at 300 °C and increased rapidly at over 400 °C until most of the CB was burned off. At 600 °C, the ΔV of the sensor element with the Ag/TiO_2 catalyst decreased because there was little residual CB. In these cases, the contact condition between the catalyst layer and the CB is indicated by the schematic in Fig. 4(b). First, some CB that had a tight contact with the catalyst (such as the TC mode) burned between 300 and 400 °C, as shown in Fig. 4(b-A). At over 400 °C, the CB that had a loose contact with the catalyst (such as the LC mode) burned, as shown in Fig. 4(b-B). Then, at 600 °C, a small amount of residual CB, which had hardly any contact with the catalyst (much looser than the LC mode), burned [Fig. 4(b-C)].

The ΔV of the sensor element with the Ag/CeO_2 catalyst began to increase at 400 °C and kept increasing rapidly until 600 °C. It is considered that CB, which had a loose contact with the catalyst [Fig. 4(b-B)], burned immediately after the combustion of CB, which had a tight contact with the catalyst [Fig. 4(b-A)]. On the other hand, the ΔV of the sensor element with the $Ag/\alpha\text{-}Al_2O_3$ catalyst hardly changed at the temperature of 450 to 550 °C and increased rapidly at 600 °C. It is considered that much of the CB on the sensor element burned at approximately 600 °C, which is close to the temperature of the natural combustion, although a small amount of CB, which had a tight contact with the catalyst [Fig. 4(b-A)], burned.

These results suggest that the contact state is different between the catalyst and the CB, which can be measured according to different sensor signals (output voltage). Moreover, it is clear that the contact state between the catalyst and the CB has a large effect on the sensing performance.

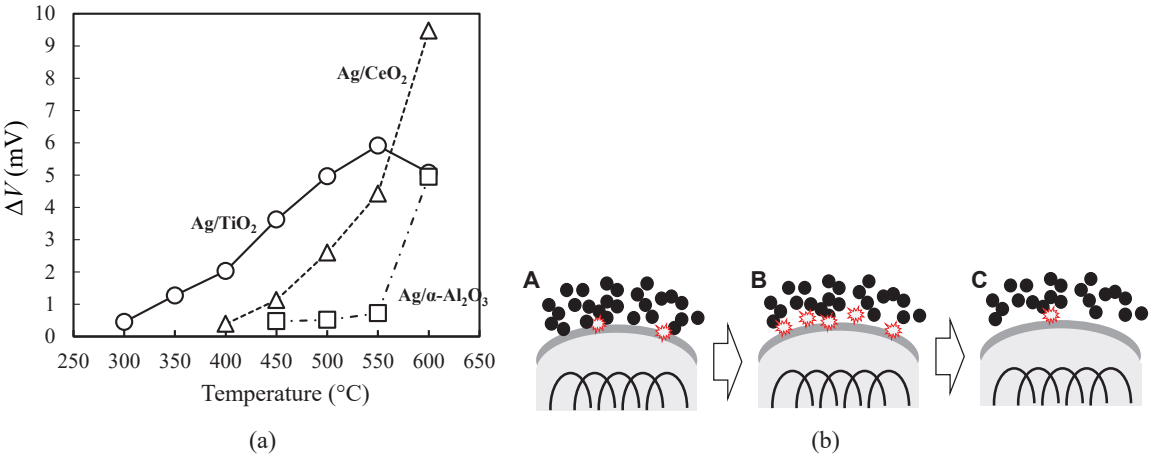

Fig. 4. (Color online) (a) Sensing performances (ΔV) for soot combustion with different catalysts at increasing temperature in air and (b) different contact modes of combustion condition.

3.3 Sensing property in exchanged gas, N_2 to air, under constant temperature

The sensing properties of the sensor elements with Ag/TiO_2, Ag/CeO_2, and $Ag/\alpha\text{-}Al_2O_3$ catalysts under constant temperature are shown in Fig. 5. The sensor element coated with the catalyst and the CB was kept in N_2 for 5 min at 600 °C and then the gas was changed to air at the same temperature. It is clear that almost all the CB coated with different catalysts had burned after changing N_2 to air. Here, the peak output voltage after changing N_2 to air is caused by the CB combustion in the TC mode, indicating that the combustion heat of CB conducted through the sensor element to the Pt coil. The increase in output voltage after that peak is caused by CB combustion in the LC mode and indicates the decrease in the amount of residual CB with high heat capacity because the combustion heat hardly conducts to the Pt coil.

In Fig. 5(a), CB coated on Ag/TiO_2 was oxidized suddenly after changing N_2 to air, and the difference in output voltage (ΔV, $\Delta V = V_{air} - V_N$, V_{air} is the output voltage in air and V_N is the output voltage in N_2) was about 10 mV during the first 5 min, and the contact condition between the catalyst and the CB was near the TC mode [Fig. 4(b-A)]. The output voltage continued to increase with time, and the contact condition between the catalyst and the CB is near the LC mode [Fig. 4(b-B)]. The residual CB continued to be burned while the output voltage increased slightly until all the CB burned out. Figure 5(b) shows the sensing property of the sensor element coated with both $Ag/\alpha\text{-}Al_2O_3$ and CB. The output voltage returned to the same level as in N_2 following a sharp oxidation peak after changing N_2 to air and then increased slowly until all the CB was consumed, thereby showing a fast combustion speed, because most of the CB was oxidized during the first 5 min. The sensing property of the sensor element coated with both Ag/CeO_2 and CB is shown in Fig. 5(c), and its output voltage gradually increased without the peak after changing N_2 to air, which was different from that of the other two sensors.

The difference in sensing properties among these sensor elements coated with different catalysts is mainly due to the different internal properties of the catalysts. To understand the relationship between the sensing properties and the oxidation performance of the CB, we evaluated the response

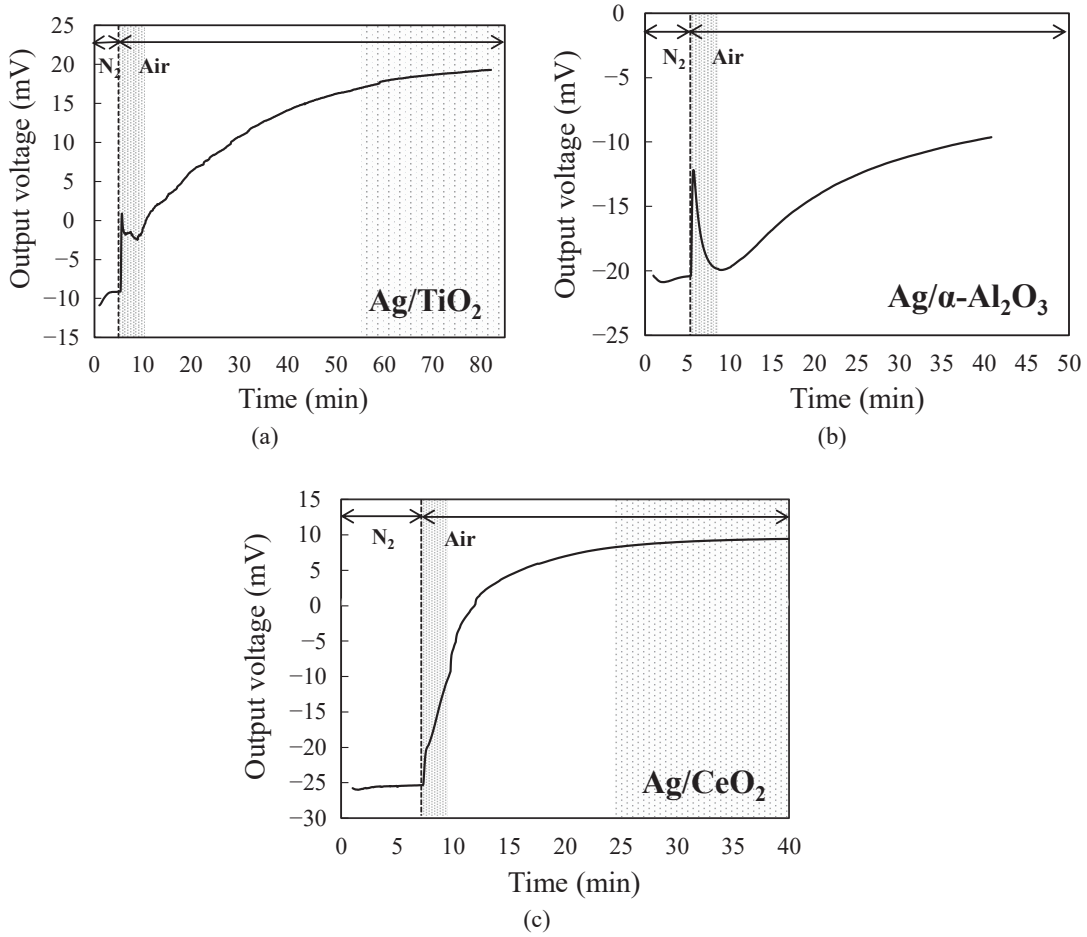

Fig. 5. Sensing performances for soot combustion with different catalysts at 600 °C for 5 min before changing N_2 to air: (a) Ag/TiO_2, (b) $Ag/\alpha\text{-}Al_2O_3$, and (c) Ag/CeO_2.

speed of the CB oxidation. The response speed of the CB oxidation at 10 and 50% of the total output voltage was denoted as V_{10} and V_{50}, respectively, as shown in Fig. 6. The total output voltage ΔV is the difference between the output voltage at which all the CB was oxidized and the output voltage in N_2 before oxidation.

Figure 7 shows the comparison of the response speeds for CB oxidation estimated from the equation described above. The response speeds V_{10} of CB oxidation were 50, 34, and 21 $mV \cdot min^{-1}$ for sensor elements with Ag/TiO_2, $Ag/\alpha\text{-}Al_2O_3$, and Ag/CeO_2 catalysts, respectively. The peak area of the output voltage after changing N_2 to air corresponds to the amount of combustion heat (ΔH). The amplitude of the estimated ΔH from Fig. 6 became large in the order of the sensor elements with Ag/TiO_2, $Ag/\alpha\text{-}Al_2O_3$, and Ag/CeO_2 catalysts. Therefore, this suggests that the catalyst with a high CB oxidation activity has a fast response speed at an early stage. On the other hand, the response speeds V_{50} of CB oxidation were 1.6, 0.7, and 17.7 $mV \cdot min^{-1}$ for sensor elements with Ag/TiO_2, $Ag/\alpha\text{-}Al_2O_3$, and Ag/CeO_2 catalysts, respectively. This suggests that the V_{50} of CB oxidation has no relation with the oxidation heat.

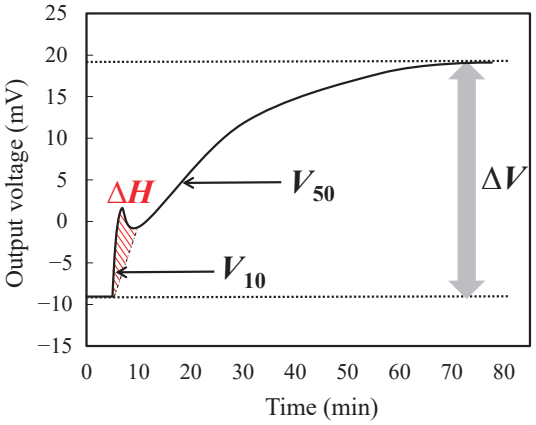

Fig. 6. (Color online) V_{10} and V_{50} of the total output voltage.

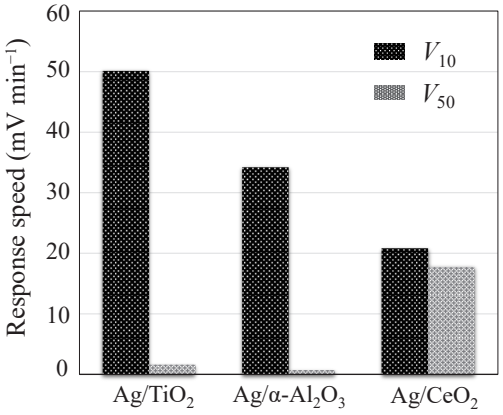

Fig. 7. Comparison of response speed (V_{10} and V_{50}) for CB sensing.

As shown in Table 1, it is clear that the catalyst with better catalytic activity in T_{max} in the TC mode had a higher response speed V_{10} for CB oxidation. However, the V_{50} for CB oxidation has no relationship with the catalytic activity in T_{max} in the LC mode. Moreover, although the response curve of the sensor element with the Ag/CeO_2 catalyst increased gradually without an obvious peak after changing the gas (from N_2 to air), its V_{50} was highest among the sensor elements with these catalysts.

In the case of the sensor element with the Ag/CeO_2 catalyst, the difference between V_{10} and V_{50} was very small compared with those of the sensor elements with Ag/TiO_2 and $Ag/\alpha\text{-}Al_2O_3$ catalysts. In addition, the difference in the CB oxidation activities of the catalysts (ΔT_{max} in Table 1) between the TC and LC modes was also consistent with the difference in the response speed between V_{10} and V_{50} (ΔV_{50-10}). For example, the difference in the response speed, ΔV_{50-10}, of the CB oxidation for the sensor element with the Ag/CeO_2 catalysts, which showed the smallest ΔT_{max} (8 °C in Table 1) for the CB combustion, was only 3.1 $mV \cdot min^{-1}$, which was much smaller than 48.5 and 33.5 $mV \cdot min^{-1}$ for the sensor elements with the Ag/TiO_2 and $Ag/\alpha\text{-}Al_2O_3$ catalysts, respectively.

These results suggest that the catalyst with the high intrinsic CB oxidation activity (T_{max} in TC mode) improves the response property (V_{10}) at an early stage. On the other hand, the catalyst that does not depend on the contact state (TC and LC modes) improves the response property of the CB oxidation at the later stage [Figs. 4(b-B) and 4(c-C)]. In this study, the best catalyst for the soot sensing is Ag/CeO_2, which showed almost the same response speed of V_{10} and V_{50}. We suggest that the close response speed of V_{10} and V_{50} is most important in the real condition, regardless of the active species and the support materials. The contact state between the catalyst and the soot is quite loose under the practical condition. Therefore, the response speed of V_{50} will become important for the catalyst used in the combustion-type PM sensor.

4. Conclusion

The soot-sensing properties of the combustion-type sensor coated with Ag-supported catalysts (Ag/TiO_2, $Ag/\alpha\text{-}Al_2O_3$, and Ag/CeO_2) were investigated. The catalyst with an intrinsically high CB oxidation activity had a high response speed although the response speed had no relationship

with the CB oxidation activity, regardless of the contact state between the catalyst and the CB. Moreover, the difference in CB oxidation activity between the TC and LC modes was consistent with the difference in the response speed between V_{10} and V_{50}. The catalyst with high intrinsic CB combustion activity improves the response property at an initial combustion. On the other hand, the catalyst having CB combustion activity which does not depend on the contact state between the CB and the catalyst, improves the response property at later combustion.

In this study, we demonstrated not only the preliminary result of the detection for the soot oxidation under operation temperature but also indicated a catalyst design for soot oxidation. However, because most of our research in this work was focused on qualitative analysis, a more quantitative evaluation of the sensing property and measurements under real exhaust conditions isnecessary in the future.

Acknowledgements

This work was supported by the Adaptable and Seamless Technology Transfer Program through target driven R&D from the Ministry of Education, Culture, Sports, Science and Technology, Japan.

References

1 J. C. Summers, S. Van Houtte, and D. Psaras: Appl. Catal., B **10** (1996) 139.
2 H. S. Rosenkranz: Mutat. Res. **367** (1996) 65.
3 C. B. Lim, H. Einaga, Y. Sadaoka, and Y. Teraoka: Sens. Actuators, B **160** (2011) 463.
4 M. Zheng, G. T. Reader, and J. G. Hawley: Energy Convers. Manage. **45** (2004) 883.
5 M. M. Maricq: J. Aerosol Sci. **38** (2007) 1079.
6 M. Ambrogio, G. Saracco, and V. Specchia: Chem. Eng. Sci. **56** (2001) 1613.
7 S. Teranishi, K. Kondo, A. Tsuge, and T. Hibino: Sens. Actuators, B **140** (2009) 170.
8 A. Vogel, V. Schüle, G. Baier, and A. Mahl: Sens. Actuators, B **18–19** (1994) 546.
9 V. Schüle, G. Baier, and A. Vogel: Sens. Actuators, B **15–16** (1993) 249.
10 G. Hagen, C. Feistkorn, S. Wiegartner, A. Heinrich, D. Bruggemann, and R. Moos: Sensors **10** (2010) 1589.
11 P. Bartscherer and R. Moos: J. Sens. Sens. Syst. **2** (2013) 95.
12 M. Feulner, G. Hagen, A. Müller, A. Schott, C. Zöllner, D. Brüggemann, and R. Moos: Sensors **15** (2015) 28796.
13 G. Fischerauer, M. Förster, and R. Moos: Meas. Sci. Technol. **21** (2010) 035108.
14 M. Feulner, G. Hagen, A. Piontkowski, A. Müller, G. Fischerauer, D. Brüggemann, and R. Moos: Top. Catal. **56** (2013) 483.
15 C. D. Litton: Fire Saf. J. **37** (2002) 409.
16 C. D. Litton: Fire Saf. J. **44** (2009) 387.
17 A. Keller, M. Rüegg, M. Forster, M. Loepfe, R. Pleisch, P. Nebiker, and H. Burtscher: Sens. Actuators, B **104** (2005) 1.
18 J. J. Murphy and C. R. Shaddix: Combust. Flame **143** (2005) 1.
19 Y. B. Shen, T. Takeuchi, S. Teranishi, and T. Hibino: Sens. Actuators, B **145** (2010) 708.
20 Y. B. Shen, T. Takeuchi, and T. Hibino: Sens. Actuators, B **153** (2011) 226.
21 Y. B. Shen, T. Harada, S. Teranishi, and T. Hibino: Sens. Actuators, B **162** (2012) 159.
22 Y. Shirashi and N. Toshima: J. Mol. Catal., A **141** (1999) 187.
23 J. P. A. Neeft, M. Makkee, and J. A. Moulijn: Fuel **77** (1998) 111.
24 A. N. Pestrvakov: Catal. Today **28** (1996) 239.
25 L. Kundakovic and M. Flytzani-Stephanopolus: Appl. Catal., A **183** (1999) 35.
26 A. Nagy and G. Mestl: Appl. Catal., A **188** (1999) 337.
27 P. W. Park and C. L. Boyer: Appl. Catal., B **59** (2005) 27.
28 R. Brosius, K. Arve, M. H. Groothaert, and J. A. Martens: J. Catal. **231** (2005) 344.

29 L. Gang, B. G. Anderson, J. van Grondelle, R. A. van Santen, W. J. H. van Gennip, J. W. Niemantsverdriet, P. J. Kooyman, A. Knoester, and H. H. Brongersma: J. Catal. **206** (2002) 60.
30 S. Imamura, H. Yamada, and K. Utani: Appl. Catal., A **192** (2000) 221.
31 Z. Qu, M. Cheng, W. Huang, and X. Bao: J. Catal. **229** (2005) 446.
32 M. Luo, X. Yuan, and X. Zheng: Appl. Catal., A **175** (1998) 121.
33 E. Aneggi, J. Llorca, C. D. Leitenburg, G. Dolcetti, and A. Trovarelli: Appl. Catal., B **91** (2009) 489.
34 G. Corro, U. Pal, E. Ayala, and E. Vidal: Catal. Today **212** (2013) 63.
35 G. Corro, U. Pal, E. Ayala, E. Vidal, and E. Guilleminot: Catal. Today **56** (2013) 467.
36 T. Itoh, M. Nishibori, E. Einaga, and Y. Teraoka: Chem. Sens. **30**, Supplement A (2014) 82.